Condensed Matter Physics.
Solid state physics

UDC 538.9

EDN CGGAPH
https://www.doi.org/10.33910/2687-153X-2026-7-2-59-64

Correlations between NMR data, Mössbauer spectroscopy data and the EFG tensor parameters for copper nodes in $RBa_2Cu_3O_{7-x}$ superconducting metal oxides

A. V. Marchenko [1], T. E. Baimirzaeva [1], V. S. Kiselev [1], P. P. Seregin ✉[1]

[1] Herzen State Pedagogical University of Russia, 48 Moika Emb., Saint Petersburg 191186, Russia

Authors

Alla V. Marchenko, ORCID: 0000-0002-9292-2541, e-mail: al7140@rambler.ru

Tamara E. Baimirzaeva, e-mail: toma4535@mail.ru

Valentin S. Kiselev, e-mail: kiselev.valentin@gmail.com

Pavel P. Seregin, ORCID: 0000-0001-5004-2047, e-mail: ppseregin@mail.ru

For citation: Marchenko, A. V., Baimirzaeva, T. E., Kiselev, V. S., Seregin, P. P. (2026) Correlations between NMR data, Mössbauer spectroscopy data and the EFG tensor parameters for copper nodes in $RBa_2Cu_3O_{7-x}$ superconducting metal oxides. *Physics of Complex Systems*, 7 (2), 59–64. https://www.doi.org/10.33910/2687-153X-2026-7-2-59-64 EDN CGGAPH

Received 13 January 2026; reviewed 3 February 2026; accepted 3 February 2026.

Funding: The study had no financial support.

Abstract. Linear ratios have been determined between the quadrupole interaction constants, measured by nuclear magnetic resonance with the ^{63}Cu isotope, emission Mössbauer spectroscopy with the ^{67}Zn isotope and the principal component of the electric field gradient tensor in the copper nodes of $RBa_2Cu_3O_7$ ceramic superconductors. These ratios make it possible to determine compounds in which copper is bivalent without using any models of charge distribution across the nodes within the crystal lattice.

Keywords: nuclear magnetic resonance, Mössbauer spectroscopy, electric field gradient tensor, high-temperature superconductors, electronic defects

Introduction

Determining the spatial distribution of electronic defects in the lattices of superconducting copper metal oxides is one of the urgent problems in the physics of high-temperature superconductivity. This problem can be effectively solved by a comparison of experimentally determined and calculated parameters of the electric field gradient (EFG) tensor for copper nodes.

Nuclear magnetic resonance (NMR) with the ^{63}Cu isotope (Asayama et al. 1996) and emission Mössbauer spectroscopy (EMS) with the ^{67}Cu parent isotope (Bordovsky et al. 2012) are the most applicable methods used to determine the EFG parameters for copper nodes. The measurement results of both methods can be presented as a quadrupole interaction constant

$$C = eQU_{zz} \quad (1)$$

and the EFG tensor asymmetry parameter

$$\eta = (U_{yy} - U_{xx})/U_{zz}, \quad (2)$$

where U_{zz}, U_{yy} and U_{xx} are the diagonalized EFG tensor components on the probe nucleus, $|U_{zz}| \geq |U_{yy}| \geq |U_{xx}|$, and Q is the quadrupole moment of the probe nucleus.

For the $^{63}Cu^{2+}$ probe, EFG on the nuclei is created by the crystalline lattice ions (crystalline EFG) and the non-spherical valence shell of the probe atom (valence EFG). When the orientations of the two tensors' principal axes coincide, then the ratio occurs

$$eQU_{zz} = eQ(1 - \gamma)\, V_{zz} + eQ(1 - R_o)\, W_{zz}, \quad (3)$$

where U_{zz}, V_{zz} and W_{zz} are total, crystalline and valence EFG tensor principal components for the $^{63}Cu^{2+}$ probe, and γ and R_0 are Sternheimer coefficients for the probe.

If EMS with the ^{67}Zn isotope obtained from the ^{67}Cu parent nuclei is used for the experimental determination of the EFG tensor parameters in copper nodes, we should take into account that zinc valence electrons do not contribute to the EFG for the $^{67}Zn^{2+}$ probe, which results in

$$eQU_{zz} \approx eQ(1 - \gamma)V_{zz}. \quad (4)$$

It is of undoubted interest to find the ratios between NMR spectroscopy data with the ^{63}Cu isotope, EMS data with the $^{67}Cu(^{67}Zn)$ isotopes and the crystalline EFG tensor principal components in order to evaluate the charge states of atoms in the superconductive lattices.

In the present work, such ratios are established between the quadrupole interaction constants for the ^{63}Cu (C_{Cu}), ^{67}Zn (C_{Zn}) nuclei and the crystal EFG tensor principal component V_{zz} for the bivalent copper nodes in the $RBa_2Cu_3O_7$ lattices (R = Nd, Sm, Eu, Gd, Y, Er, Tm,Yb), as well as for the monovalent copper nodes in the $YBa_2Cu_3O_6$, Cu_2O and $Nd_{1.85}Ce_{0.15}CuO_4$ lattices, making it possible to evaluate the validity of charge distribution models for crystal lattices of high-temperature superconductors.

Experimental methodology

The $RBa_2Cu_3O_{7-x}$ samples were prepared using the ceramic technology with the ^{67}Cu isotope, obtained by the $^{67}Zn(n, p)^{67}Cu$ reaction irradiating ^{67}ZnO with fast reactor neutrons, followed by the chromatographic detachment of the carrier-free $^{67}CuCl_2$ preparation. The $RBa_2Cu_3O_7$ control samples had a superconducting phase transition temperature within the 75–85 K range and a rhombohedral structure, while the $YBa_2Cu_3O_6$ control samples did not display a transition to the superconducting state up to 4.2 K and had a tetragonal structure.

$Nd_{1.85}Ce_{0.15}CuO_4$ ceramics were synthesized by sintering the corresponding oxides in the air at 1,120 °C, followed by annealing in argon at 900 °C. The ^{67}Cu radioactive isotope was injected into ceramics by diffusion alloying at 900 °C for an hour. The control samples were single-phase, and T_c = 22 K was obtained for the $Nd_{1.85}Ce_{0.15}CuO_4$ ceramics. Copper nitrous oxide was obtained by decomposition of the copper nitrate.

The ^{67}Zn Mössbauer spectra were recorded at 4.2 K with the ^{67}ZnS absorbers (1,000 mG/cm^2).

The ^{63}Cu NMR data for $RBa_2Cu_3O_{7-x}$ were taken from (Matsumura et al. 1998; Pennington et al. 1989; Takatsuka et al. 1991), for Cu_2O from (de Wijn, de Wildt 1966), and for $Nd_{1.85}Ce_{0.15}CuO_4$ from (Kambe et al. 1991).

The crystalline EFG tensors in the copper sites within the $RBa_2Cu_3O_{7-x}$, $YBa_2Cu_3O_6$, $Nd_{1.85}Ce_{0.15}CuO_4$ and Cu_2O lattices were calculated according to the point charges approximation. The $RBa_2Cu_3O_{7-x}$, $YBa_2Cu_3O_6$, $Nd_{1.85}Ce_{0.15}CuO_4$ and Cu_2O lattices were represented as a superposition of sublattices

$$\begin{gathered} RBa_2Cu(l)Cu(2)_2O(l)_2O(2)_2O(3)_2O(4), \\ YBa_2Cu(1)Cu(2)_2O(1)_2O(2)_2O(3)_2, \\ (Nd_{1.85}Ce_{0.15})CuO_4, \\ Cu_4O_2, \end{gathered} \quad (5)$$

and the tensor components for the node were written as the sum of the contributions from the individual sublattices

$$V_{\alpha\alpha} = \sum_k e_k^* \sum_n \frac{1}{r_{ki}^3}\left(3\frac{\alpha_{kn}^2}{r_{kn}^2} - 1\right) = \sum_k e_k^* G_{\alpha\alpha k}\ ,$$

 https://www.doi.org/10.33910/2687-153X-2026-7-2-59-64

$$V_{\alpha\beta} = \sum_k e_k^* \sum_n \frac{3\alpha_{kn}\beta_{kn}}{r_{kn}^5} = \sum_k e_k^* G_{\alpha\beta k} \ , \tag{6}$$

where k is the summation index over the sublattices k = 1 – Y, k = 2 – Ba, k = 3 – Cu1, k = 4 – Cu2, k = 5 – O1, k = 6 – O2, k = 7 – O3, k = 8 – O4, n is the summation index over the sublattice nodes, α, β are the Cartesian coordinates, r_{kn} is the distance from the k_n ion to the lattice site under consideration, and e^*_k is the effective charge of the atoms in the k-sublattice.

To calculate the crystalline EFG tensor for the $RBa_2Cu_3O_7$ series and for $YBa_2Cu_3O_6$, the atom position in the unit cell and the unit cell parameters were used according to (Le Page et al. 1987; Tarascon et al. 1987). While calculating the EFG tensor in the copper nodes of the Cu_2O lattice, the atom coordinates within the unit cell and the unit cell parameters were used from (Wells 1984). For the $Nd_{1.85}Ce_{0.15}CuO_4$ lattice, the atom coordinates in the elementary cell and the lattice constants were used according to (Sadowski et al. 1990).

Results and discussion

Figs. 1 and 2 display experimental data for the values of the quadrupole interaction constant for the ^{63}Cu nuclei in the Cu1 ($|C_{Cu1}|$) and Cu2 ($|C_{Cu2}|$) nodes of the $RBa_2Cu_3O_7$ lattices, as well as in the copper ($|C_{Cu+}|$) nodes of the Cu_2O, $YBa_2Cu_3O_6$ and $Nd_{1.85}Ce_{0.15}CuO_4$ lattices obtained by NMR with the ^{63}Cu [3–12] and EMS with the ^{67}Cu(^{67}Zn) (our original data), in the form of $|C_{Cu1}| = f(C_{Zn})$, $|C_{Cu2}| = f(C_{Zn})$ and $|C_{Cu+}| = f(C_{Zn})$ dependencies.

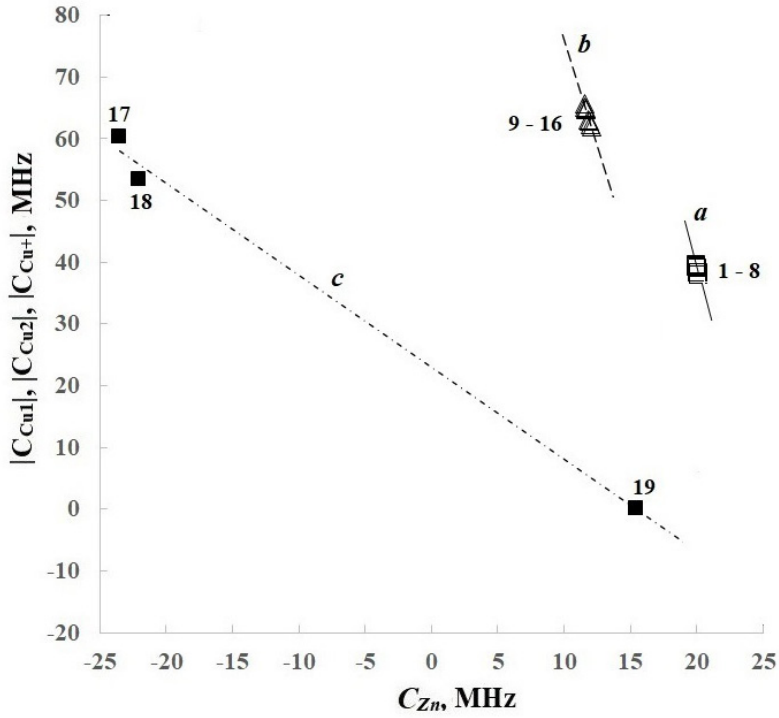

Fig. 1. Experimental dependences $|C_{Cu1}| = f(C_{Zn})$, $|C_{Cu2}| = f(C_{Zn})$ and $|C_{Cu+}| = f(C_{Zn})$. The $|C_{Cu1}|$, $|C_{Cu2}|$ and $|C_{Cu}|$ data were obtained by NMR with the ^{63}Cu [3–12], and the C_{Zn} data were obtained by EMC with the ^{67}Cu(^{67}Zn). Here $|C_{Cu1}|$, $|C_{Cu2}|$ and $|C_{Cu+}|$ are the quadrupole interaction constants for the ^{63}Cu centers in copper nodes, and C_{Zn} are the quadrupole interaction constants for the ^{67}Zn centers in copper nodes. Designations: Cu1 in $NdBa_2Cu_3O_7$ (1), $SmBa_2Cu_3O_7$ (2), $EuBa_2Cu_3O_7$ (3), $YBa_2Cu_3O_7$ (4), $GdBa_2Cu_3O_7$ (5), $ErBa_2Cu_3O_7$ (6), $TmBa_2Cu3O_7$ (7), $YbBa_2Cu_3O_7$ (8), $NdBa_2Cu_3O_7$ (9), $SmBa_2Cu_3O_7$ (10), $EuBa_2Cu_3O_7$ (11), $YBa_2Cu_3O_7$ (12), $GdBa_2Cu_3O_7$ (13), $ErBa_2Cu_3O_7$ (14), $TmBa_2Cu_3O_7$ (15), $YbBa_2Cu_3O_7$ (16), Cu1 in $YBa_2Cu_3O_6$, (17) Cu in Cu_2O (18) and Cu in $Nd_{1.85}Ce_{0.15}CuO_4$ (19)

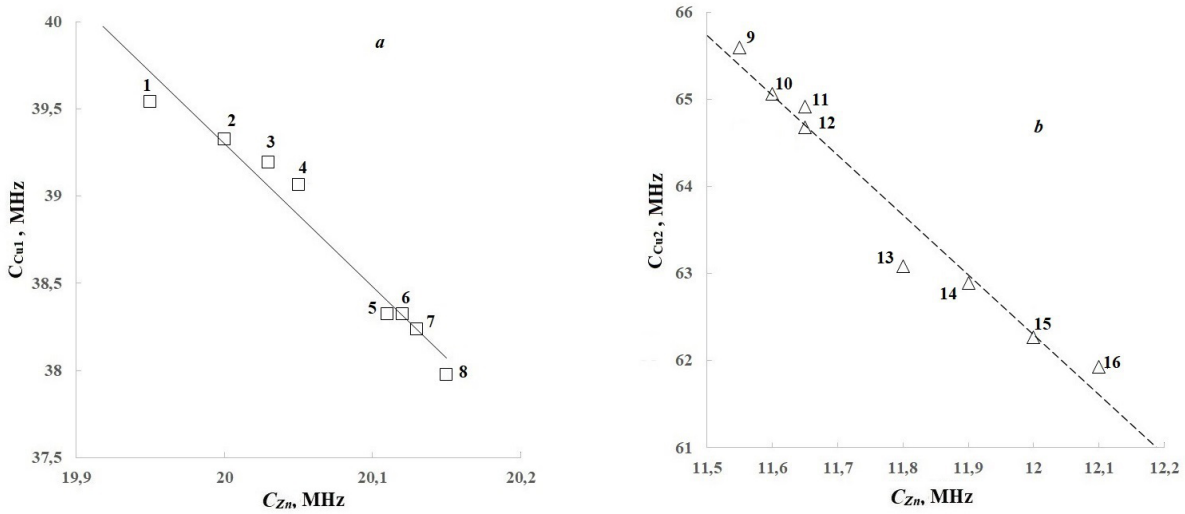

Fig. 2. Experimental dependencies $|C_{Cu1}| = f(C_{Zn})$ (*a*) and $|C_{Cu2}| = f(C_{Zn})$ (*b*) in an enlarged scale

It can be seen that the data corresponding to the bivalent copper compounds are located on two different linear dependences corresponding to the Cu1 and Cu2 centers,

$$|C_{Cu1}| = -8.21\ C_{Zn} + 203.6, \tag{7}$$

$$|C_{Cu2}| = -9.93\ C_{Zn} + 181.2, \tag{8}$$

and what is more is that these dependences differ from the dependence obtained for the Cu+ single-phase copper centers

$$|C_{Cu+}| = -1.49\ C_{Zn} + 23, \tag{9}$$

which is characterized by an insignificant contribution to the EFG for the ^{63}Cu nuclei from the valence electrons (all values in (7–9) are indicated in MHz).

It should also be concluded that the contribution from the valence electrons to the total EFG for the ^{63}Cu nuclei is the same for both Cu1 [$eQ(1 - R)W_{zz} \sim 204$ MHz] and Cu2 [$eQ(1 - R)W_{zz} \sim 145$ MHz] centers in all the studied compounds. At the same time, a decrease in $|C_{Cu1}|$ and $|C_{Cu2}|$ with an increase in C_{Zn} is evidence for the opposite signs of the valence and crystalline contributions in formula (1) and leads to the ratio

$$|(1 - R)W_{zz}| > |(1 - \gamma)V_{zz}| \tag{10}$$

for bivalent copper centers in $RBa_2Cu_3O_7$.

The dependences $|C_{Cu1}| = f(C_{Zn})$ and $|C_{Cu2}| = f(C_{Zn})$ and ratios (7, 8) can be used to select the compounds in which copper is bivalent and for which the directions of the principal axes of the valence and crystalline EFG tensors coincide. Such a selection does not use any models of charge distribution along the nodes of the crystal lattice.

Fig. 3 and Fig. 4 shows the dependences $|C_{Cu1}| = f(V_{zz})$ and $|C_{Cu2}| = f(V_{zz})$, which are similar to the dependences $|C_{Cu1}| = f(C_{Zn})$ and $|C_{Cu2}| = f(C_{Zn})$ since C_{Zn}, according to (2), is proportional to V_{zz}. When calculating V_{zz}, the choice of a model of charge distribution across the lattice sites is of fundamental importance. The best agreement with the experiment is shown by models

$$\mathbf{R^{3+}Ba_2^{1.98+}Cu(1)_2^{2.04+}Cu(2)_2^{2.1+}O(1)_2^{2.06-}O(2)_2^{1.99-}O(3)_2^{1.88-}O(4)^{1.32-}} \tag{11}$$

$$\mathbf{Nd_{1.85}^{3.075+}Ce_{1.85}^{3.075+}Cu^{1.85+}O_4^{2-}} \tag{12}$$

$$\mathbf{Y^{3+}Ba_2^{2+}Cu(1)_2^{2+}Cu(2)_2^{2+}O(1)_2^{2-}O(2)_2^{2-}O(3)_2^{2-}} \tag{13}$$

$$\mathbf{Cu_4^{+}O_2^{2-}}. \tag{14}$$

 https://www.doi.org/10.33910/2687-153X-2026-7-2-59-64

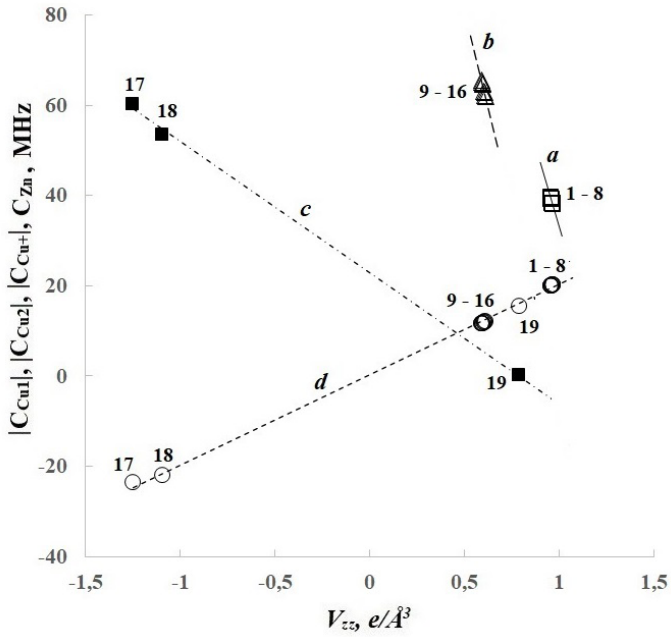

Fig. 3. Experimental dependences $|C_{Cu1}| = f(V_{zz})$, $|C_{Cu2}| = f(V_{zz})$, $|C_{Cu+}| = f(V_{zz})$ and $C_{Zn} = f(V_{zz})$. The $|C_{Cu1}|$ and $|C_{Cu2}|$ data were obtained by NMR with the ^{63}Cu [3–12], and the C_{Zn} data, by EMS with the ^{67}Cu(^{67}Zn). Here V_{zz} is the crystalline EFG tensor principal component

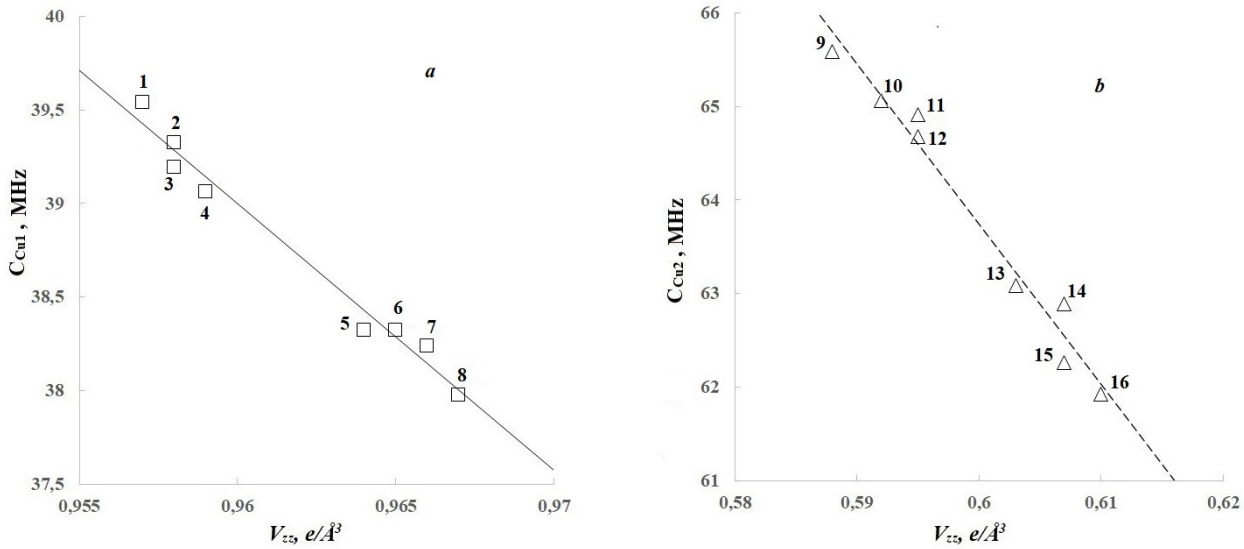

Fig. 4. Experimental dependences $|C_{Cu1}| = f(V_{zz})$ (*a*) and $|C_{Cu2}| = f(V_{zz})$ (*b*) in an enlarged scale

It can be seen that the data corresponding to the bivalent copper compounds are still located on two linear dependences corresponding to Cu1 and Cu2

$$|CCu1| = -142.5V_{zz} + 175.8, \tag{15}$$

$$|CCu2| = -176.1V_{zz} + 170, \tag{16}$$

and once more these dependences differ from the dependence obtained for Cu+ monovalent copper centers by a small contribution to the total EFG on ^{63}Cu nuclei

$$|CCu+| = -29.1V_{zz} + 23. \tag{17}$$

This difference is especially noticeable in the case of the bivalent zinc centers, for which the contribution to the total EFG from valence electrons, firstly, coincides in sign with the crystalline EFG, and, secondly, the contribution from valence electrons is very small

$$C_{Zn} = 20V_{zz} + 0.24. \quad (18)$$

In formulas (15–18), the values of $|C_{Cu1}|$, $|C_{Cu2}|$, $|C_{Cu+}|$ and C_{Zn} are given in MHz, and the values of V_{zz} are in e/Å^3.

The ratios (15, 16) can be used to evaluate the reliability of the proposed model charge distributions within the lattice sites for superconductive ceramics.

Conclusion

Thus, linear dependences between $|C_{Cu}|$ (NMR data with the ^{63}Cu) and C_{Zn} (EMS data with the ^{67}Cu(^{67}Zn)) for bivalent copper metal oxides are demonstrated, which indicates the similarity of the copper electronic structure in these lattices. A similar linear dependence is found between $|C_{Cu}|$ (NMR data with the ^{63}Cu) and V_{zz} (calculated in the point charge model approximation), which can be used to evaluate the reliability of the proposed model charge distributions within the lattice sites for superconductive ceramics.

Conflict of Interest

The authors declare that there is no conflict of interest, either existing or potential.

Author Contributions

The authors have made an equal contribution to the preparation of the paper.

References

Asayama, K., Kitaoka, Y., Zheng, G.-Q., Ishida, K. (1996) NMR studies of high T_c superconductors. *Progress in Nuclear Magnetic Resonance Spectroscopy*, 28 (3–4), 221–253. https://doi.org/10.1016/0079-6565(95)01025-4 (In English)

Bordovsky, G. A., Seregin, P. P., Marchenko, A. V. (2012) *Mössbauer of negative U centers in semiconductors and superconductors. Identification, properties, and application*. Saarbrücken: LAP LAMBERT Academic Publ., 508 p. (In English)

De Wijn, H. W., de Wildt, J. L. (1966) Temperature dependence of nuclear quadrupole resonance in cuprous oxide. *Physical Review*, 150 (1), 200–201. https://doi.org/10.1103/PhysRev.150.200 (In English)

Kambe, S., Yasuoka, H., Takagi, H. et al. (1991) ^{63,65}Cu-NMR study of oxidized and reduced $Nd_{2-x}Ce_xCuO_4$. *Journal of the Physical Society of Japan*, 60 (2), 400–403. https://doi.org/10.1143/JPSJ.60.400 (In English)

Le Page, Y., Siegrist, T., Sunshine, S. A. et al. (1987) Structural properties of $Ba_2RCu_3O_7$ high-T_c superconductors. *Physical Review B*, 36 (7), 3617–3621. https://doi.org/10.1103/PhysRevB.36.3617 (In English)

Matsumura, M., Shiohara, T., Yamagata, H. (1998) Cu-NQR study in the paramagnetic state in $YBa_2Cu_3O_6$. *Journal of the Physical Society of Japan*, 67 (9), 3267–3274. (In English)

Pennington, C. H., Durand, D. J., Slichter, C. P. et al. (1989) Static and dynamic Cu NMR tensors of $YBa_2Cu_3O_{7-\delta}$. *Physical Review B*, 39 (4), 2902–2905. https://doi.org/10.1103/PhysRevB.39.2902 (In English)

Sadowski, W., Walker, E., Francois, M. et al. (1990) Growth of single crystals, thermal dependency of lattice parameters and Raman scattering in the $Nd_{2-x}Ce_xCuO_4$ system. *Physica C: Superconductivity*, 170 (1-2), 103–111. (In English)

Takatsuka, T., Kumagai, K., Nakajima, H., Yamanaka, A. (1991) Hyperfine fields and quadrupole frequencies at each Cu site in $RBa_2Cu_3O_6$ and $RBa_2Cu_3O_7$ (R: rare-earth element). *Physica C: Superconductivity*, 185–189 (2), 1071–1072. (In English)

Tarascon, J. M., McKinnon, W. R., Greene, L. H. et al. (1987) Oxygen and rare-earth doping of the 90-K superconducting perovskite $YBa_2Cu_3O_{7-x}$. *Physical Review B*, 36 (1), 226–234. https://doi.org/10.1103/PhysRevB.36.226 (In English)

Wells, A. F. (1984) *Structural Inorganic Chemistry*. 5th ed. Oxford: Oxford University Press, 1382 p. (In English)